AUTONOMOUS AERIAL RENDEZVOUS OF SMALL UNMANNED AIRCRAFT SYSTEMS USING A TOWED CABLE SYSTEM

Joseph Nichols and Liang Sun
Multiple Agent Intelligent Coordination and Control (MAGICC) Laboratory
Brigham Young University, Provo, Utah 84602

ABSTRACT

Many unmanned aircraft systems (UAS) have relatively short endurance and range which limits their usefulness in applications where their home station is a long distance from the area of interest. This paper lays out a method for placing a towed drogue system into an appropriate orbit used by a seeker UAS to track and rendezvous with it. The principle contributions of the work include a method for controlling the drogue path by manipulating the mothership orbit and airspeed. Another contribution is a vision-based nonlinear tracking method that provides pitch rate and roll commands to allow the seeker UAS to rendezvous with the drogue. Flight test results are presented to demonstrate the suitability of these methods.

INTRODUCTION

Autonomous aerial rendezvous for small UAS enables the availability of the technology in air-to-air interception applications like aerial refueling and aerial recovery **[1].** A notional aerial recovery system would consist of a larger vehicle to transport the UAS to the area of interest, launch them, and subsequently autonomously retrieve them by deploying a high-drag drogue that will allow the UAS to match angular velocity of the mothership, but at a much lower airspeed. The approach taken in this work is to employ a drogue towed by a flexible cable attached to a mothership, as shown in Figure 1. The minimum velocity of the mothership is assumed to be much faster than the maximum velocity of the UAS which necessitates a flexible cable system that will place the drogue in an orbit inside the mothership orbit and at a velocity achievable by the UAS.

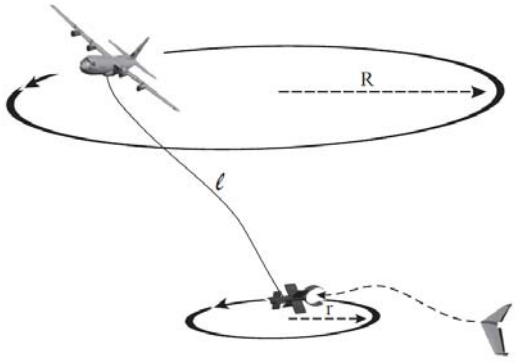

Figure 1 -- Aerial recovery concept. The mothership tows a drogue that is pulled into an interior orbit to facilitate UAS-drogue rendezvous and docking.

SYSTEM DESCRIPTION

The hardware system used to test the control algorithms developed during this project consisted of four elements—a seeker UAS, a mothership UAS to tow the drogue, a passive towed drogue, and a ground station. These elements as shown in Figure 2.

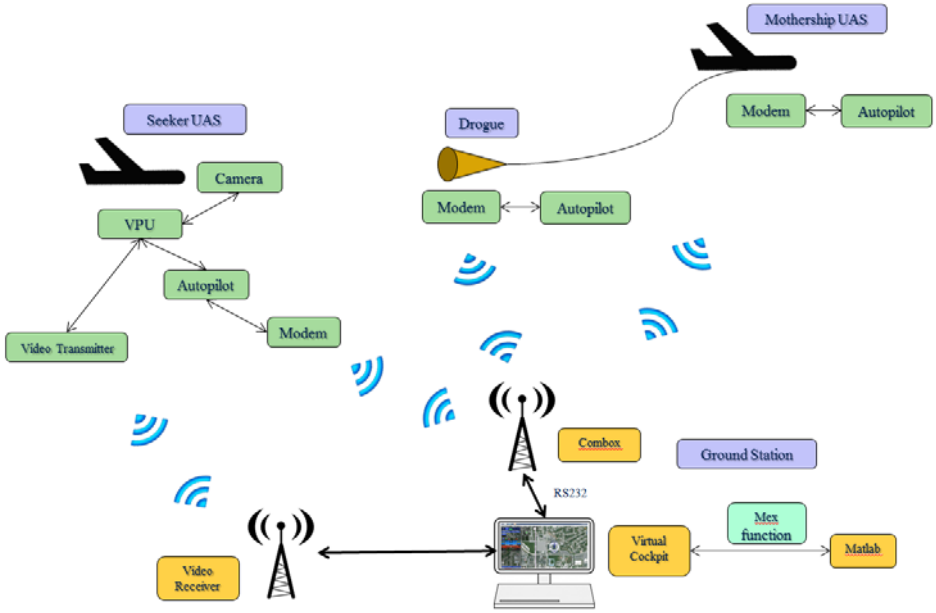

Figure 2 – Aerial Recovery System Description

Seeker UAS

The rendezvous methods were tested with a seeker UAS following a target UAS. The 1.4 m wingspan seeker UAS shown in Figure 3 was equipped with a Kestrel 2 autopilot **[2]** and a separate processor for interfacing with the camera called the vision processing unit (VPU) **[3].** The Kestrel 2 autopilot contains an onboard inertial measurement unit that is used to estimate the vehicle state. A GPS unit provides position data. Standard remote controlled (RC) plane servos and a motor controller were used to power the vehicle. The autopilot used an antenna to communicate with a communications relay on the ground. The communications relay interfaced with the user ground station. The ground station sent high-level commands to the autopilot and VPU as well as received real-time vehicle telemetry. For our tests, the high-level commands allowed us to switch between tracking the target UAS using the camera image or tracking the GPS location of the target through the communications relay. The seeker UAS control algorithm discussed in this paper was implemented onboard the VPU. The VPU communicated with the autopilot over a serial port. This allowed the VPU to receive autopilot telemetry packets and to send command packets to the autopilot at 30 Hz. In our tests we used the autopilot pitch rate control loop, the airspeed control loop, and the roll angle control loop. Thus, when implemented onboard the VPU, our interception and tracking algorithms produced desired airspeed, roll angle, and pitch rate commands which were then sent to the autopilot.

A digital camera was used in conjunction with the VPU. The fixed camera was mounted in the nose of the seeker UAS and had a 78 degree field of view. Visual tracking techniques programmed onto the VPU made it possible to manually designate and track user selected

airborne targets. The video feed was transmitted to the ground and displayed in the ground station. The user manually selected a target in the video feed that the UAS was commanded to track and follow.

(a) Seeker UAS

(b) Mothership UAS and Drogue

(c) Kestrel 2 Autopilot

(d) Vision Processing Unit (VPU)

Figure 3 – Flight Hardware.

Mothership UAS

The 1.4 m wing span mothership was powered by two 770 Watt battery-operated motors. The mothership was equipped with a Kestrel 2 autopilot and modem to communicate with the ground station **[2].** It was modified with a controlled release for the drogue cable. The UAS was hand launched and was landed on its belly autonomously or manually by the safety pilot. A photograph of the aircraft can be seen in Figure 3b and the autopilot in Figure 3c. The mothership control algorithms discussed in this paper were implemented in Matlab and run on the desktop computer in the ground station.

Drogue

The 30-cm-diameter hemisphere drogue used in this project was constructed of reinforced plastic as shown in Figure 3b. The drogue was equipped with a Kestrel 2 autopilot **[2]** and modem for reporting its position and velocities to the ground station. The drogue GPS states were rebroadcast to the seeker UAS. The drogue was passive and had no controllable surfaces and it was attached to the mothership with a 100 m cable made of fishing line of 20 lb. maximal load.

Ground Station

The ground station was a desktop computer with interfaces to the autopilot communications relay and the video relay. The computer ran a software application called Virtual Cockpit 3D (VC3D) which is a standard interface for the Kestrel autopilot and allowed the operator to monitor the status of all three autopilots simultaneously. VC3D also allowed the operator to

communicate with the VPU onboard the seeker UAS to pass target designation information and allow the operator to change pursuit modes. The communications link with the autopilots was 115.2 KB/second which included all three vehicles. In addition, the desktop computer had Matlab installed to run the control algorithms for the mothership control. The ground station was housed in a portable trailer with a generator and work areas for maintaining the aircraft.

CONTROLLING THE MOTION OF A TOWED CABLE SYSTEM

In a perfect windless environment, a horizontal flat orbit flown by the mothership drives the drogue to converge to a horizontal flat orbit with a smaller radius than that of the mothership orbit. However in the presence of wind, the drogue orbit becomes an inclined ellipse as shown in Figure 4. This figure illustrates the system trajectories in the presence of 4 m/s wind coming from the east. The altitude deviation of the drogue orbit was more than 20 meters over the course of an orbit in relatively mild winds. For winds around 10 m/s the altitude deviation has been observed to exceed 50 m over the period of one orbit. For the seeker UAS to successfully rendezvous with the drogue, a flatter orbit is desired. Therefore, a strategy to maintain a flat and circular drogue orbit in the presence of wind is needed to achieve a successful aerial rendezvous.

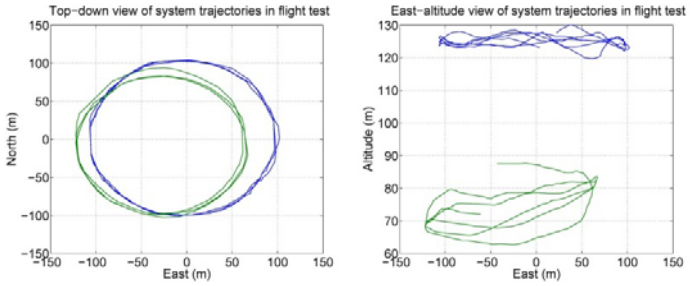

Figure 4 -- Drogue and mothership trajectories in the presence of 4 m/s wind.

Equations of Motion

We have seen that for flexible cable systems like we have used in this project, the cable stretches considerably **[4].** An elastic model for the cable is therefore needed to match simulation results to flight results. In this paper, we develop the cable-drogue dynamics using an elastic model based on Newton's second law. Figure 5 depicts a cable-drogue system as an n-link cable modeled as finite number of point mass nodes connected by springs. The forces acting on each link are lumped together and applied at the joint. The drogue is the last joint of the cable.

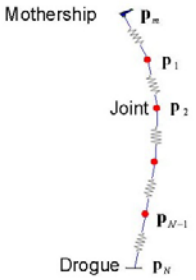

Figure 5 – Cable-drogue systems using spring model

From Newton's second law, equations of motion of the drogue and each joint are given by

$$m_i\ \ddot{p}_j\ = T_j\ +\ G_j\ +\ D_j\ + L_j\ -\ T_{j+1}, j = 1, 2, \dots, n-1. \quad (1)$$

For each joint: m is the mass, p is the position in the inertial frame, T is the tension, G is the gravitational force, L is the lift force, and D is the drag force.

Mothership Trajectory Generation

The concept of differential flatness has proved useful for path planning for complex nonlinear systems **[5]**. We make use of the differential flatness property of the cable-drogue system to calculate the inverse dynamics relating a desired drogue orbit to the required orbit of the mothership. Assuming that the only forces on the drogue are aerodynamic forces, gravity, and tension forces from the cable, the cable-drogue system is differentially flat using the trajectory of the drogue as a flat output. Therefore, specifying the desired trajectory of the drogue will dictate the required trajectory for each cable link, and, consequently, for the mothership. For a smooth trajectory, the tension components in the Nth link of the cable (at the end attached to the drogue) from

$$T_N\ =\ m_n\ \ddot{p}_n\ -(G_n\ +\ D_n\ + L_n). \quad (2)$$

The stretched length of jth link lj can be calculated by

$$l_j\ = l_0\left(1 + \frac{\|T_j\|}{EA}\right), j = 2, 3, \dots, n, \quad (3)$$

where ‖ ‖ denotes the Euclidean norm and E is Young's modulus and A is the cross-sectional area of the cable. Then the location of the (j-1)th point mass is related to the jth point mass using

$$p_{j-1}\ =\ p_j + \ l_j\ \frac{T_j}{\|T_j\|}. \quad (4)$$

Consequently, the forces on the (j-1)th point mass can be calculated by

$$T_{j-1}\ =\ m_{j-1}\ \ddot{p}_{j-1}\ -\left(G_{j-1}\ +\ D_{j-1}\ + L_{j-1}\right) +\ T_j\,. \quad (5)$$

At each time step, these equations are applied recursively to each link of the cable until the trajectory of the mothership is calculated.

A typical drogue orbit can be used to derive the desired mothership trajectory. Let $p^d(t) \triangleq \left(p^d_{north}, p^d_{east}, p^d_{down}\right)$ be the position of the drogue in North-East-Down coordinates in the inertial frame, r^d is the desired constant radius of the drogue, θ is the orbital angle which is defined in Figure 6 for clockwise motion, and h_0 is the desired constant altitude of the drogue. Assuming the center of the drogue orbit lies at the origin, the desired circular trajectory of the drogue can be written as

$$p^d_{north}\ =\ r^d\ \cos\theta\,(t) \quad (6)$$
$$p^d_{east}\ =\ r^d\ \sin\theta\,(t) \quad (7)$$

$$p^d_{down} = -h_0 \tag{8}$$

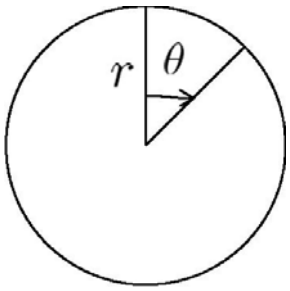

Figure 6 -- Desired drogue trajectory with radius (r) and orbital angle (θ).

Let $v(t)$ be the velocity vector of the drogue in the wind frame, $w(t) \triangleq (w_{north}, w_{east}, w_{down})$ be the wind vector in the North-East-Down coordinates in the inertial frame, and the first and second order derivatives of $p^d(t)$ with respect to time are given by

$$\dot{p^d} = \begin{pmatrix} -r^d\,\dot{\theta}\cos\theta \\ r^d\,\dot{\theta}\sin\theta \\ 0 \end{pmatrix} = v + w \tag{9}$$

$$\ddot{p}^d = \begin{pmatrix} -r^d\,(\ddot{\theta}\sin\theta + \dot{\theta}^2\cos\theta) \\ r^d\,(\ddot{\theta}\cos\theta - \dot{\theta}^2\sin\theta) \\ 0 \end{pmatrix}. \tag{10}$$

Thus, given the desired r^d, h_0, $\theta(t)$, and a prediction of the wind vector w, we can apply the differential flatness based strategy to derive the desired trajectory for the mothership.

Waypoint Generation and Tracking

Given a desired trajectory of the mothership, one applicable approach to achieve the navigation and control of the autopilot is to send a commanded airspeed, course angle and altitude through Virtual Cockpit (VC3D) every step (0.2 s in the flight test). However, the altitude following belongs to the higher level control and expresses a lag in response which makes the actual altitude of the mothership unable to reach the peaks or troughs during the flight. Another available method of still using the mex function communicating with Virtual Cockpit is to send an appropriate commanded waypoint with its airspeed to VC3D, which turns out to work very well. The first step is to generate a series of waypoints using the desired mothership trajectory. Since the differential flatness based calculation is a numerical method, that is, the results of the desired mothership trajectories are already discretized points. Therefore a strategy is needed to convert these points into a set of applicable waypoints which are sent to the VC3D from MATLAB through the mex function.

Given the current position of the mothership, the procedure of computing the commanded waypoint is as follows:

1. Given a desired drogue motion pattern, using differential flatness, we numerically calculate the discrete points of desired mothership trajectory in one orbit circle.
2. The center coordinates of the desired mothership orbit is calculated by averaging the coordinates of the points on the orbit.

3. The orbit angle θ of each point on the orbit with respect to the calculated center is then calculated. With round-off in the unit of degree and is wrapped within the range (-180 – 180 degrees).
4. A look-up table was established with θ ascending sorted in the first column and the corresponding desired coordinates in three dimensions, and airspeed in the successive columns.
5. Removing the rows with duplicates of θ, we obtain a look-up table with 361 rows ascending sorted in θ.
6. Given the current position of the mothership, we calculate its orbit angle θ_p with respect to the center. Defining $\theta_c \triangleq \theta_p + \lambda\, \delta_\theta$, where $\lambda = 1$ signifies a clockwise orbit and $\lambda = -1$ signifies a counterclockwise orbit, and δ_θ is a constant integer that is decided by trial and error. Then a waypoint on the desired orbit of the mothership corresponding to the orbit angle θ_c is selected and sent to VC to update the commanded waypoint.

CONTROL OF THE SEEKER UAS

The seeker UAS must acquire, track and navigate to the location of the orbiting drogue. Our initial efforts involved calculating a vector field based on the estimated elliptical path of the drogue and commanding the seeker UAS to follow this path **[6]**. This allowed us to keep the seeker UAS in loose formation with the drogue while we developed the vision-based control methods. Distance from the drogue was controlled using proportional/integral (PI) control of the airspeed using the difference from the desired separation distance as the error. A linear pursuit method was implemented using PI control with good results, but the best tracking results were obtained by using the Lyapunov-based nonlinear control method described in this section.

The relative lateral dynamics between the seeker UAS and the drogue are described in polar coordinates in the seeker UAS body frame shown in Figure 7.

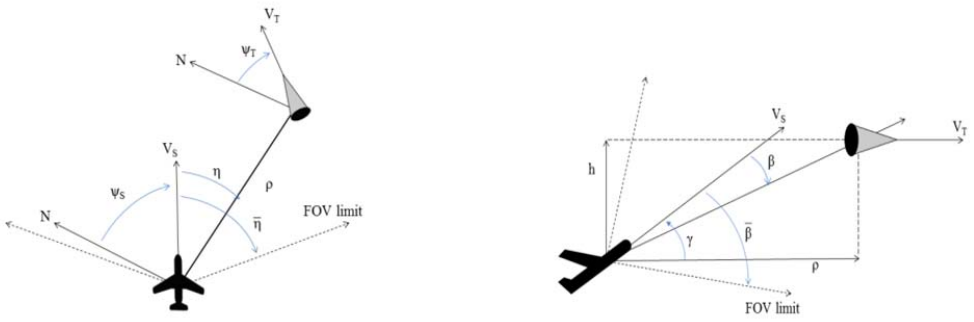

(a) Lateral Dynamics (b) Longitudinal Dynamics

Figure 7 – Relative dynamics between the seeker UAS and the drogue.

The lateral and longitudinal dynamics as shown in Figure 7 are

$$\dot{\psi}_S = \frac{g}{V_S} \tan\phi \tag{11}$$

$$\dot{\rho} = V_T\, cos(\psi_S - \psi_T + \eta) - V_S \cos\eta \tag{12}$$

$$\dot{\eta} = -\dot{\psi}_S + \frac{V_S}{\rho}\sin\eta + \frac{V_T}{\rho} sin(\psi_S - \psi_T + \eta) \tag{13}$$

$$\dot{\beta} = \frac{-(V_T - V_S \cos\gamma)\, \sin(\gamma+\beta) - V_S \sin\gamma \cos(\gamma+\beta)}{\rho} - \dot{\gamma}. \tag{14}$$

Heading change rate ($\dot{\psi}_S$) is computed from a standard relationship with bank angle (ϕ) **[7].** The line of sight vector (ρ) is the distance between the seeker and the towed drogue projected onto the horizontal plane. The drogue is assumed to be flying at a constant altitude and constant velocity. The azimuth and elevation line-of-sight rates are $\dot{\eta}$ and $\dot{\beta}$ respectively.

To find a nonlinear control law that can be proven to drive the line-of-sight errors to zero we introduce two Lyapunov function candidates $W_{lateral} = \frac{1}{2}\eta^2$, and $W_{longitudinal} = \frac{1}{2}\beta^2$. By choosing commanded values for ϕ and $\dot{\gamma}$ such that all the nonlinear terms become zero leaving only the line-of-sight rate multiplied by a gain, the first derivative of the scalar functions become $\dot{W}_{lateral} = -K_\phi\, \eta^2$ and $\dot{W}_{longitudinal} = -K_\gamma\, \beta^2$. The derivatives of these functions are negative definite and therefore the controls ϕ^c and $\dot{\gamma}^c$ are guaranteed to drive the elevation and azimuth line-of-sight errors to zero **[8].** The nonlinear control of roll and pitch rate were determined to be

$$\phi^c = \tan^{-1}\left(\frac{V_S}{g}\left(\frac{V_S}{\rho}\sin\eta + \frac{V_T}{\rho} sin(\psi_S - \psi_T + \eta) + K_\phi\eta\right)\right), \tag{15}$$

$$\dot{\gamma^c} = \frac{-(V_T - V_S \cos\gamma)\, \sin(\gamma+\beta) - V_S \sin\gamma \cos(\gamma+\beta)}{\rho} + K_\gamma\beta, \tag{16}$$

where K_ϕ and K_γ are experimentally determined gains.

Line-of-sight angles were determined from the pixel location of the target designated by the ground station operator. When no target was designated, the line-of-sight angles were calculated based on the GPS position of the drogue and converted into the body frame. An extended Kalman filter was used to estimate the drogue location between GPS updates (5 Hz update rate). The pixel location of the target is the center of the green acquisition box around the drogue indicating lock on that is shown in Figure 8.

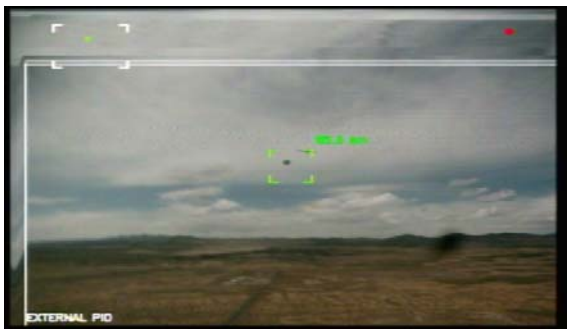

Figure 8 – A video frame from the seeker UAS camera showing the drogue and the user selected tracking point in the green box.

ACHIEVING AIRBORNE RENDEZVOUS

Airborne rendezvous was achieved by initiating distance closure by increasing the seeker UAS airspeed by an operator chosen increase over the drogue airspeed (typically 2 m/s). This was accomplished when the seeker UAS had a good visual track of the drogue. The nonlinear control algorithm was used to control the UAS during the approach to rendezvous. As the seeker UAS approached the drogue, gains were reduced as a function of distance to the drogue to limit large control oscillations. When the seeker UAS sensed that it had passed the half plane location of the drogue it reduced airspeed to retreat and reinitiate following the drogue from 25 m and then reinitiate the rendezvous attempt.

FLIGHT TEST RESULTS

Drogue Orbit Control

It can be seen from Figure 9a that the mothership performed well in following the airspeed and altitude commands calculated by the waypoint generation and tracking algorithm. In Figure 9b we can see that the waypoint following strategy works well in manipulating the mothership to follow the desired orbit. It can be seen from Figure 9c that this method works well in flattening the drogue orbit in the presence of wind. However, a strategy of updating the desired mothership orbit based on the change of the wind is needed.

To update the desired mothership orbit based on the change of the wind, we cannot apply the traditional instant feedback strategy because the towed cable system is a not rigid body, which means that the cable connection delays the response the drogue motion when the motion pattern of the mothership changes. In this paper, we updated the desired mothership orbit once per orbit based on the change of wind estimation and we assume that the wind will not change within each orbit.

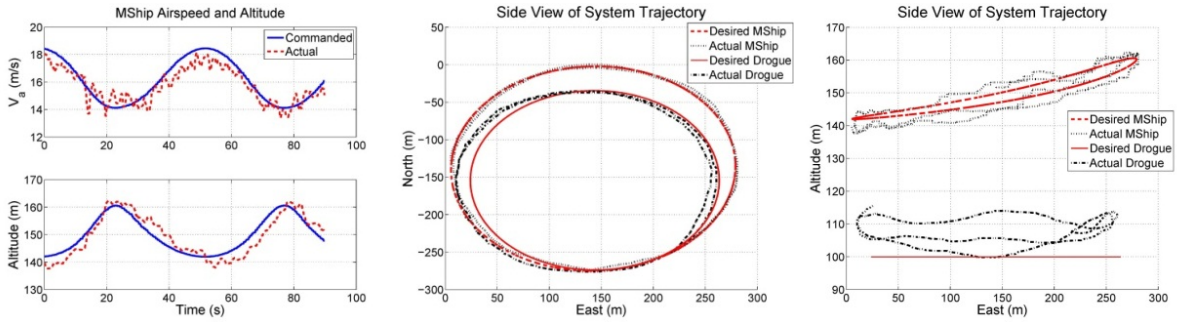

(a) (b) (c)

Figure 9 – Results using the desired drogue orbit with constant ground speed.

Tracking

The nonlinear tracking method was tested against the mothership directly flying without the drogue. The target vehicle (mothership) was flown in the pattern shown in Figure 10. Wind was 9 m/s from the south. The flight pattern allowed for left and right hand turns into the wind. The line-of-sight rate data shown in Figure 9 is based on the GPS position of the target. The onboard camera had a field of view of 78 degrees. Therefore the line of sight angle must remain within +/- 0.6835 radians to remain in the camera field of view. The results in Figure 10

confirm that the target was kept within the camera field of view throughout the aggressive maneuver in high winds.

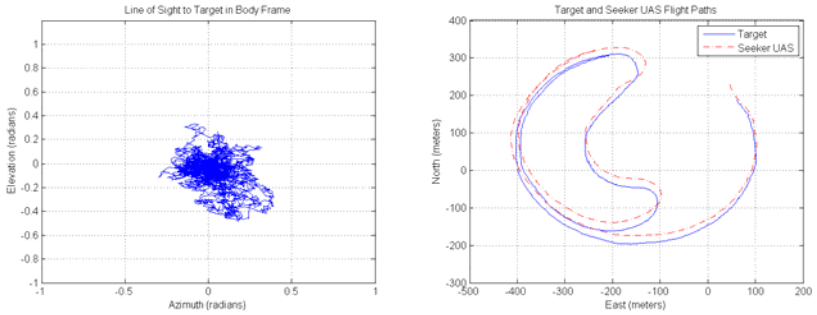

Figure 10 – Tracking Test Results.

Rendezvous

The full system was tested by the mothership pulling the drogue on a 100 m cable and the seeker UAS tracking and then locking on and attempting to touch the drogue. Numerous attempts were made during the program. Typically the seeker UAS was commanded to follow the target from a distance of 20-30 m. When stable behind the target and with a good visual lock, the engage command was given which then commanded the seeker UAS to use the nonlinear line-of-sight algorithm fed with vision data to close on the drogue. The seeker airspeed was commanded to be typically 2 m/s faster than the measured drogue airspeed. An example engagement is shown in Figure 11. It can be seen in Figure 11c that the seeker UAS lost lock on the drogue three times during the engagement and its closest approach was 2.7 m. Maintaining visual lock on the target throughout the engagement proved to be a difficult challenge throughout the test program. Nevertheless, when locked onto the target, the control method worked well to keep the target in the field of view as can be seen in Figure 11a. When not visually locked on to the drogue, the seeker UAS used the GPS position of the drogue to feed the control algorithm. While we did succeed in hitting the target during the program, we could not do it consistently. Approaches within a few meters like the example shown were common.

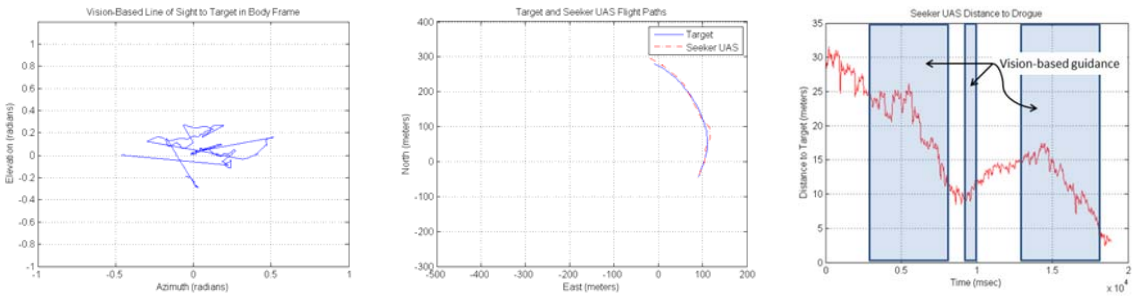

(a) (b) (c)

Figure 11 – Flight test results of the seeker UAS closing on the drogue

LESSONS LEARNED

Small UAS testing requires the same test discipline as full-scale flight testing **[9],** but the team is generally smaller and each person must be a master of several disciplines.

For multi-agent operations the test team must pay particular attention to the communications bandwidth. Look for non-essential data that is taking large amounts of bandwidth. We experienced large communications lags with flight controls that could only be corrected by reducing the update rate of some less essential sensors.

Launching a small UAS with a towed drogue is best accomplished by a single loop of the cable and then launching the mothership on a heading 90 degrees from the layout of the cable. This minimizes the potential of tangling the cable and allows the mothership to gain sufficient altitude and airspeed to pull the drogue up into the air avoiding low obstacles.

CONCLUSIONS

Algorithms were developed and flight tested which demonstrated the feasibility of aerial rendezvous. The ability to control a non-maneuvering drogue orbit through control of the mothership airspeed and flight path was demonstrated. We demonstrated a method for using a camera to obtain the line-of-sight to the target and the ability to track the lateral and longitudinal motion of the target and keep it within the camera field of view. Finally we demonstrated a method to combine the above to close on the target and consistently pass within a few meters of the drogue. Future work should include the development of a more robust vision tracker, increasing the stability of the drogue, and extending the nonlinear flight control methods.

ACKNOWLEDGEMENTS

Research support for this work was provided by the Air Force Office of Scientific Research through the Small Business Technology Transfer Program, contract number FA9550-10-C-0041, and in cooperation with Lockheed Martin Procerus Technologies. This support is gratefully acknowledged.

REFERENCES

[1] M.B. Colton, L. Sun, D.C. Carlson, and R.W. Beard. Multi-vehicle dynamics and control for aerial recovery of micro air vehicles. Int. J. Vehicle Autonomous Systems, 9:78107, 2011.

[2] Lockheed Martin Procerus Technologies. http://www.procerusuav.com/productsKestrelAutopilot.php.

[3] Lockheed Martin Procerus Technologies. http://www.procerusuav.com/Downloads/DataSheets/VPU_DataSheet_2011_01_26.pdf.

[4] Liang Sun and Randal W. Beard. Towed body altitude stabilization and state estimation in aerial recovery of micro air vehicles. AIAA, Guidance, Navigation and Control Conference, Toronto, Ontario, Canada, August 2010.

[5] Michel Fliess, Jean Levine, Philippe Martin, and Pierre Rouchon. Flatness and defect of non-linear systems: introductory theory and examples. *International Journal of Control*, 61(6):1327-1361, 1995.

[6] Joseph W. Nichols, Jeff Ferrin, Mark Owen, and Tim McLain. Vision-Enhanced Aerial Rendezvous along Elliptical Paths. AIAA, Guidance, Navigation and Control Conference, Minneapolis, Minnesota, August 2012.

[7] Randal W. Beard and Timothy W. McLain. *Small Unmanned Aircraft: Theory and Practice*. Princeton University Press, 2012.

[8] Hassan K. Khalil. *Nonlinear Systems*. Prentice Hall, 2002.

[9] John L. Minor, David P. Warner, 1st Lt Javier Hurtado Jr, Nathan L. Cook, Lt Col Russell G. Adelgren, and Capt Jason C. Doster. Lessons learned during development of a hands-on unmanned aerial vehicle flight test and evaluation training course. SFTE 36th Annual International Symposium, Fort Worth, Texas, October 2005.

AUTHOR BIOGRAPHIES

Joseph Nichols is a Ph.D. student in the Department of Mechanical Engineering at Brigham Young University studying control of unmanned aircraft systems. He received a Bachelor of Science degree from Brigham Young University in mechanical engineering and a Master of Science degree from the United States Air Force Institute of Technology in aeronautical engineering. Mr. Nichols spent 26 years in the U.S. Air Force primarily working in test and evaluation. Mr. Nichols is a graduate of the U.S. Air Force Test Pilot School and he is a member of SFTE. Mr. Nichols can be reached at nichols@byu.edu.

Liang Sun received his Bachelor of Science and Master of Science degrees from Beihang University, China, in 2004 and 2007, respectively. He is currently a Ph.D. student in the Department of Electrical and Computer Engineering at Brigham Young University. His research areas include: cooperative control of unmanned air vehicles, nonlinear control, dynamic modeling, trajectory tracking, path following, and backstepping. Mr. Sun can be reached at liang.sun@byu.edu.